IEEE Access
Multidisciplinary | Rapid Review | Open Access Journal

Received January 25, 2018, accepted February 18, 2018, date of publication March 5, 2018, date of current version May 16, 2018.

Digital Object Identifier 10.1109/ACCESS.2018.2811838

An Efficient CSI Feedback Scheme for Dual-Polarized Massive MIMO

FENG ZHENG[1], YIJIAN CHEN[2], BOWEN PANG[3], CHEN LIU[1], SHICHUAN WANG[1], DEWEN FAN[1], AND JIE ZHANG[4]

[1]Beijing Key Laboratory of Network System Architecture and Convergence, Beijing University of Posts and Telecommunications, Beijing 100876, China
[2]ZTE Corporation, Shenzhen 518055, China
[3]International School, Beijing University of Posts and Telecommunications, Beijing 100876, China
[4]Department of Electronic and Electrical Engineering, The University of Sheffield, Sheffield S102TN, U.K.

Corresponding author: Feng Zheng (zhengfeng@bupt.edu.cn)

This work was supported by the National Science and Technology Major Project of China under Grant 2017ZX03001004.

ABSTRACT As an effective solution to the tradeoff between array size and the number of antenna elements, dual-polarization antenna is widely utilized in massive MIMO systems. However, the existing channel state information (CSI) feedback schemes are not suitable for dual-polarized massive MIMO as they ignore the polarization leakage between the polarization directions, causing significant performance degradation. To facilitate accurate channel acquisition, this paper proposes a practical channel model for dual-polarized massive MIMO by taking polarization leakage into consideration. The model formulates the channel as the sum of two components, i.e., the ideal polarization channel and the polarization leakage channel between the polarization directions. Based on the channel model, the eigenvector structures of both the ideal polarization channel and the polarization leakage channel are analyzed. Moreover, two novel CSI feedback schemes are also designed, i.e., explicit feedback scheme (EFS) and implicit feedback scheme (IFS). In EFS, the parameters determining the eigenvectors of the two channels are fed back explicitly, while the two channels are fed back using predetermined codebook in IFS. Extensive link level and system level simulations are conducted to validate the performance of the proposed schemes and the results show that they significantly outperform the existing CSI feedback schemes.

INDEX TERMS Dual polarization antenna, massive MIMO, CSI feedback, polarization leakage.

I. INTRODUCTION

The fifth generation mobile communication (5G) is targeting ubiquitous, high speed, low latency, highly flexible wireless communication for a wide spectrum of applications including enhanced mobile broadband (eMBB), massive machine type of communication (mMTC) and ultra-reliable and low-latency communications (URLLC) [1]. One prominent goal of 5G is to significantly improve the capacity of current wireless networks. For this purpose, several technologies including ultra-dense networks (UDN) and millimeter wave communication (MWC), are proposed [2]. Among them, massive MIMO is widely viewed as a key component of 5G as it can enable efficient spectrum sharing by serving multiple user equipment (UE) simultaneously using low complexity linear precoding schemes [3]–[5]. Moreover, massive MIMO is also compatible with many other key 5G technologies such as UDN and MWC.

The performance of massive MIMO depends on antenna scale and the accuracy of channel state information (CSI). Given a form factor, the number of antenna elements is inversely proportional to antenna spacing. A minimum spacing should be kept between adjacent antenna elements to avoid correlation but small array size is preferred in practical deployment. As antennas with different polarization directions are uncorrelated even if they are deployed at the same spot, dual-polarized antenna is a good solution to the tradeoff between the number of antennas and array size, and thus is widely used in massive MIMO.

Another crucial factor for the performance for massive MIMO is the accuracy of CSI. In massive MIMO systems, CSI is usually estimated at the receiver and fed back to the transmitter [6], which uses CSI for various purposes such as scheduling and precoding. In long-term evolution (LTE), the CSI feedback contains a channel quality index (CQI), a rank index (RI) and a precoding matrix index (PMI) [7]. CQI indicates the preferred modulation scheme and code rate, RI shows the rank of the MIMO channel, and PMI provides the preferred precoding matrix out of a pre-defined set of

2169-3536 © 2018 IEEE. Translations and content mining are permitted for academic research only.
Personal use is also permitted, but republication/redistribution requires IEEE permission.
See http://www.ieee.org/publications_standards/publications/rights/index.html for more information.

matrices [7]. In closed-loop MIMO systems, inaccurate CSI can result in severe degradation of the beamforming gain, as the interference among layers and users is cannot be fully canceled.

For CSI acquisition, limited feedback techniques are commonly used in massive MIMO (e.g. [8]–[11]), in which eNodeB acquires CSI based on the PMI feedback of UE. The most essential problem in limited feedback techniques is the design of the codebook, which contains all possible PMIs. The codebook needs to be small to reduce feedback overhead but also to describe the channel condition accurately for good performance. There are two methods for codebook design. One is Grassmanian line/subspace packing, which utilizes information from the connection between Grassmannian line packing and quantized beamforming to find constructive methods for designing codebooks [12]–[14], Another is to adapt vector quantization (VQ) techniques in source coding and send only the index of the codeword, which achieves significant compression [15], [16].

For dual-polarized massive MIMO systems, the codebook is typically designed based on an analysis of the channel model to match the channel characteristics. For example, an efficient Grassmannian quantization codebook is designed based on the sequential smooth optimization on the Grassmannian manifold in [17]. Zhu *et al.* and Leung *et al.* used the discrete Fourier transformation (DFT) to match the phase difference in codebook design, as the DFT-based beamforming weight vector is considered simple and effective for spatially correlated channels [18], [19]. Some researchers address the problem of codebook design for correlated channels using the statistical information about the spatial correlation among the antennas to reduce feedback overhead [20]–[23]. Antenna polarization is also considered explicitly in the design of codebook in [24]–[26], which has became the conventional choice of massive MIMO deployment. LTE-A analyzes the feature of polarized channel, and a set of codewords are derived to match the ideal dual-polarized channel [25], [26]. However, to the best of our knowledge, there is no existing research on the codebook design for imperfect dual-polarized massive MIMO.

In this paper, a model for imperfect dual-polarized channel is formulated, which treats the channel as a combination of the ideal polarization channel and the polarization leakage channel. Based on the channel model, the influence of polarization leakage on CSI feedback is analyzed. The optimal channel feature vectors and precoding weights for imperfect dual-polarized channel are derived, and two novel feedback schemes are proposed. In the explicit feedback scheme (EFS), parameters determining the eigenvectors of the ideal polarization channel and the polarization leakage channel are fed back explicitly through quantization. In the implicit feedback scheme (IFS), the ideal polarization channel and the polarization leakage channel are fed back using predetermined codebook. Extensive simulations are conducted to validate the performance of the proposed feedback schemes.

Our contributions are three-fold. The first is a general model for imperfect dual-polarized channel, which could provide insights for the design of feedback schemes. The second is the two feedback schemes based on the detailed analysis of the characteristics of imperfect dual-polarized channel. Lastly, we conduct extensive simulation to validate the performance of the proposed feedback shemes.

The remainder of the paper is organized as follows. Section II introduces the system model. The quantization efficiency of existing codebooks is analyzed in Section III and the model of imperfect dual-polarized channel is formulated in Section IV. Section V presents our two feedback schemes, i.e., EFS and IFS. Simulation results are presented in Section VI while Section VII concludes the paper.

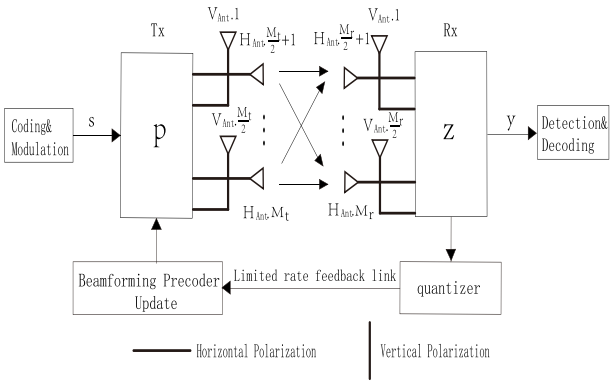

FIGURE 1. An illustration of a $M_r \times M_t$ dual-polarized MIMO system.

II. SYSTEM MODEL

Considering a MIMO system which employs transmit beamforming and receive combining respectively, the transmitter and receiver utilize M_t transmit antennas and M_r receive antennas, respectively. As dual-polarized antennas are used, M_t and M_r are assumed to be even numbers. The antenna configuration is shown in Fig.1, where the V_{Ant} denotes antennas with vertical (V) polarization and H_{Ant} denotes antennas with horizontal (H) polarization. Besides vertical and horizontal polarization, other polarization modes, such as $(+/-45)$ degrees are also possible as long as the two polarization directions are orthogonal. On transmitter side, the data symbols s are precoded with p and transmitted via polarized antennas along with the pilot signals. On the receiver side, the channel matrix is estimated from the pilot signals and the optimal precoding matrix is obtained accordingly. The optimal precoding matrix is then quantized and fed back to the transmitter via the feedback link with limited capacity. The transmitter uses this precoding matrix for the next transmission.

$$y = \sqrt{\rho} z^* \mathbf{H} \mathbf{p} s + \mathbf{z}^* n \tag{2.1}$$

We assume the fading is flat, which means the channel is constant in the considered frequency range. Note that this assumption generally holds as we can divide the working

band of the system into sub-bands and feedback a CSI for each sub-band independently. The channel matrix can be modeled by the input-output relation from V to V, V to H, H to H, and H to V polarized waves.

We can express the received signal y at the receiver as:

where $\mathbf{z}^*$ is the M_r-dimension unit-norm receive combining vector at UE, $\mathbf{p}$ is the M_t-dimension unit-norm beamforming vector at evolved Node B (eNodeB), $\mathbf{n}$ is the M_r dimension noise vector, which contains independent and identically distributed (i.i.d.) entries of Gaussian noise, s is the transmitted symbol with unit energy $E_s(ss^H) = 1$ and ρ is signal to noise ratio (SNR). Channel $\mathbf{H}$ is a dual-polarized MIMO channel parameterized by a parameter κ [10], the cross polarization power ratio in linear scale, which can be expressed as

$$\mathbf{H} = \mathbf{H}_w \bullet \mathbf{X} \tag{2.2}$$

where $\bullet$ denotes the Hadamard product between two matrices. $\mathbf{H}_w \in C^{M_r \times M_t}$ denotes the single-polarized channel, which models a channel with no power imbalance between the polarization directions. $\mathbf{X} \in C^{M_r \times M_t}$ is a matrix describing the power imbalance between the orthogonal polarization directions, which is determined by parameter $\kappa \in (0, 1)$. κ is the inverse of the Cross-Polarization Discrimination (XPD), and XPD $\in (1, +\infty)$. XPD is a ratio between the co-polarized average received power and the cross-polarized average received power. The relation between $\mathbf{X}$ and κ can be formulated as

$$\mathbf{X} = \begin{bmatrix} 1 & \sqrt{\kappa} \\ \sqrt{\kappa} & 1 \end{bmatrix} \bigotimes \begin{bmatrix} 1 & \cdots & 1 \\ \vdots & \ddots & \vdots \\ 1 & \cdots & 1 \end{bmatrix}_{M_r \times M_t} \tag{2.3}$$

Where $\bigotimes$ denotes the Kronecker product between two matrices. If $\mathbf{H}_w$ is modeled based on channel rays and the UE is assumed stationary, the channel between an arbitrary antenna pair (u, s) can be expressed as (2.4), which is derived by extending the channel model in [27] to 3D.

$$\begin{aligned} \mathbf{H}_{u,s,n}(t) = \sqrt{P_n} \sum_{m=1}^{M} & \begin{bmatrix} F_{rx,u,V}(\varphi_{n,m}, \gamma_{n,m}) \\ F_{rx,u,H}(\varphi_{n,m}, \gamma_{n,m}) \end{bmatrix}^{\mathrm{T}} \\ & \times \begin{bmatrix} \exp(j\Phi_{n,m}^{vv}) & \sqrt{\kappa}\exp(j\Phi_{n,m}^{vh}) \\ \sqrt{\kappa}\exp(j\Phi_{n,m}^{hv}) & \exp(j\Phi_{n,m}^{hh}) \end{bmatrix} \\ & \times \begin{bmatrix} F_{tx,x,V}(\phi_{n,m}, \theta_{n,m}) \\ F_{tx,x,H}(\phi_{n,m}, \theta_{n,m}) \end{bmatrix} \cdot \exp(j2\pi\lambda_0^{-1}\bar{r}_s \cdot \bar{\Phi}_{n,m}) \\ & \times \exp(j2\pi\lambda_0^{-1}\bar{r}_u \cdot \bar{\Psi}_{n,m}) \end{aligned} \tag{2.4}$$

where n denotes the index of clusters and m denotes the index of rays. $\varphi_{n,m}$ and $\gamma_{n,m}$ are the horizontal and vertical angle of arrival for ray m in cluster n, respectively. $\phi_{n,m}$ and $\theta_{n,m}$ denote the horizontal and vertical departure angle at ray m in cluster n. $F_{rx,u,V}$ and $F_{rx,u,H}$ are the antenna gain in the vertical and horizontal polarization directions and they are functions of $\varphi_{n,m}$ and $\gamma_{n,m}$. d_s and d_u are the uniform distances (m) between transmitter antenna elements and receiver antenna elements, respectively. λ_0 is the wavelength of the carrier frequency. $\exp(j\Phi_{n,m}^{vv})$ and $\exp(j\Phi_{n,m}^{hh})$ denote the random phase of each ray in the vertical and horizontal polarization direction, whereas $\exp(j\Phi_{n,m}^{vh})$ and $\exp(j\Phi_{n,m}^{hv})$ denote the random phase of polarization leakage. 1×3 vectors $\bar{\mathbf{r}}_u$ and $\bar{\mathbf{r}}_s$ denote the coordinates of the transmit and receive antennas in the space. $\bar{\mathbf{\Phi}}_{n,m}$ and $\bar{\mathbf{\Psi}}_{n,m}$ are the vectors of the Angle-of-Arrival (AoA) and Angle-of-Departure (AoD). P_n denotes the power of the n-th ray.

For the received signal in (2.1), we assume the maximal-ratio combiner (MRC) is adopted at the receiver, which uses $\mathbf{z}^* = (\mathbf{H}p)^H / \|\mathbf{H}p\|$ and maximizes the SNR γ given by (2.5).

$$\gamma = \sqrt{\rho}\|\mathbf{H}p\|^2 \tag{2.5}$$

To maximize γ, codebook design can be formulated as

$$p^{opt} = E\{\arg\max_{p \in CB} \|\mathbf{H}p\|_F^2\} \tag{2.6}$$

Currently most researches assume that there is no polarization leakage between the polarization directions, which means $\kappa = 0$. Without polarization leakage, the cross-correlation of the channel is block-diagonal, which is the basis of many feedback designs. The cross-correllation matrix of highly-correlated channel and non-correlated channel under dual-polarized massive MIMO are analyzed in [25] and [26], which shows they are far from block-diagonal.

The assumption of no polarization leakage is highly impractical. Typical XPR is between 7.2dB and 8dB, which means κ is between -7.2dB and -8dB [28]. In [29], it is reported that the outdoor to indoor (O2I) polarization leakage of the 3D-UMi and 3D-UMa channel follow Gaussian distribution with a mean of 9dB and standard deviation of 11dB. Polarization leakage can damage the characteristics of the eigenvectors, making existing channel model fail to match the eigenvectors. Therefore, when designing codebooks for dual-polarized channel, polarization leakage should be considered.

III. CODEWORD MODEL FOR PERFECT DUAL-POLARIZED CHANNEL

For an ideal polarization channel with $\kappa = 0$, the analysis in [25] and [26] shows that $\mathbf{H}^H\mathbf{H}$ is block diagonal. Specifically, for ideal correlated channel, we have $\mathbf{H}^H\mathbf{H} = \begin{bmatrix} \mathbf{A} & \mathbf{O} \\ \mathbf{O} & \mathbf{A} \end{bmatrix}$; whereas for non-ideal correlated channel, we have $\mathbf{H}^H\mathbf{H} = \begin{bmatrix} \mathbf{A} & \mathbf{B} \\ \mathbf{B} & \mathbf{A} \end{bmatrix}$, where A and B are $(M_t/2) \times (M_t/2)$ matrices, and O is all zero matrix. Therefore, for ideal polarization channel, the eigenvectors can be expressed as $\begin{bmatrix} v_i & v_j \\ \alpha v_i & -\alpha v_j \end{bmatrix}$ or $\begin{bmatrix} v_i & 0 \\ 0 & v_j \end{bmatrix}$, where $\mathbf{v}_i$ and $\mathbf{v}_j$ are $(M_t/2) \times 1$ vectors, and α is a complex number whose magnitude is 1. If the channel is highly-correlated line-of-sight channel, we have $\mathbf{v}_i = \mathbf{v}_j$, which are DFT vectors when the BS antenna is uniform linear array (ULA). If the channel is not highly correlated, $\mathbf{v}_i = \mathbf{v}_j$ still holds, but they are the weighted combinations of several DFT vectors. The higher the correlation among the channels, the smaller the chord distance between $\mathbf{v}_i$ and $\mathbf{v}_j$ will be,

and vice versa. As demonstrated by equation (2.6), when codeword matches the feature of dual-polarized channel, high SNR can be achieved. We use the chord distance to measure how well the codeword matches the channel, which is defined as follows

$$d = \frac{1}{\sqrt{2}}\|vv^H - v'(v')^H\|_F = \frac{1}{\sqrt{2}}\sqrt{tr[(vv^H - v'(v')^H)(vv^H - v'(v')^H)^H]} \quad (3.1)$$

The performance of ideal polarized channel model can degrade severely due to polarization leakage. When M_t is small, the performance degradation caused by polarization leakage is negligible as the beam generated by precoding or beamforming is wide. As M_t increases, the beam becomes narrower. If the eigenvector model derived from ideal dual-polarized array is employed for codebook design, the performance degradation can be significant.

We demonstrate the performance of the codeword based on the aforementioned eigenvector model with simulations. We set Tx antenna number as 32 and 64, and Rx antenna number as 2. Moreover, we set XPR=5dB, i.e., $\kappa = -5$dB. The quantization performance is evaluated by the chord distance (d) between the codeword and the real channel eigenvector. d=0 corresponds to the case in which there is no quantization error. We assume that there is no overhead limit for the feedback of $\mathbf{v}_i$, $\mathbf{v}_j$ and α. The CDF of d is shown in Fig.2.

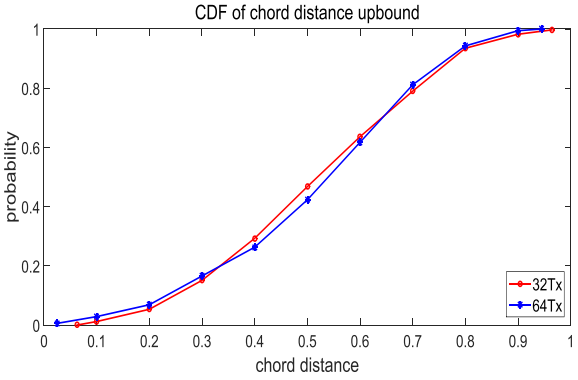

FIGURE 2. The CDF of the upper bound of the chord distance.

The results show that for 32 Tx, the probability that the chord distance between the codeword and the channel eigenvector is larger than 0.5 is approximately 53%, whereas the probability is 60% for 64 Tx. These results reveal the large quantization error of the aforementioned codeword. As d=0.5 means a 3dB loss in beamforming gain, the SNR γ can be degraded by more than 3dB. XPR=5dB is just a typical value, the κ can be much larger in practice which suggests more severe performance degradation. In conclusion, the performance of the feedback model can be significantly degraded if polarization leakage is ignored. Thus we need a channel model and feedback scheme that take polarization leakage into consideration.

IV. MODEL FOR IMPERFECT DUAL-POLARIZED CHANNEL

We consider a $N_t \times 2$ massive MIMO system which is mostly typical in practice as UE does not have enough space to hold more antennas at low frequency. The transmitter is typically (+45/−45) degree dual-polarized, and the receiver is (90/0) degree dual-polarized. According to the channel model in (2.4), the frequency domain channel matrix can be formulated as (4.1) under the assumption of flat fading

$$\mathbf{H} = \sum_{n=1}^{N}\sum_{m=1}^{M} e^{-j2\pi f_i \tau_{n,m}}\mathbf{A}_{n,m} \times (\mathbf{P}(xz_{n,m}) \otimes \mathbf{v}_{\theta_{n,m}}) \quad (4.1)$$

where $e^{-j2\pi f_i \tau_{n,m}}$ is the coefficient corresponding to the channel delay, f_i denotes the carrier frequency, $\tau_{n,m}$ denotes the delay of a path and $A_{n,m}$ denotes the amplitude of that path. $\mathbf{v}_{\theta_{n,m}}$ is a vector determined by the Tx antenna topology, which models the phase relationship among antennas caused by multiple path fading. For typical ULA, $\mathbf{v}_{\theta_{n,m}}$ is a DFT vector which can be expressed as follows

$$\mathbf{v}_{\theta_{n,m}} = [1, e^{j2\pi d\cos(\theta_{n,m})}, \ldots, e^{j(\frac{N_t}{2}-1)2\pi d\cos(\theta_{n,m})}] \quad (4.2)$$

where d is the ratio between antenna spacing and wave length, and $\theta_{n,m}$ is the azimuth angle of the path.

When the transmit antenna is a $N_{t,v}$ vertical and $N_{t,h}$ horizontal dual-polarized antenna with $N_{t,v} \times N_{t,h} \times 2 = N_t$ elements, $\mathbf{v}_{\theta_{n,m}}$ is the Kronecker product of two DFT vectors, whose beam direction depends on the azimuth and vertical angle of the path as follows

$$\mathbf{v}_{\theta_{n,m}} = [1, e^{j2\pi d\cos(\theta_{n,m})}, \ldots, e^{j(N_{t,v}-1)2\pi d\cos(\theta_{n,m})}] \otimes [1, e^{j2\pi d\cos(\phi_{n,m})}, \ldots, e^{j(N_{t,h}-1)2\pi d\cos(\phi_{n,m})}] \quad (4.3)$$

where $\phi_{n,m}$ is the vertical angle of the path.

$\mathbf{P}(xz_{n,m})$ models the random phase and projection between the polarization directions of the Rx and Tx antennas.

$$\mathbf{P}(xz_{n,m}) = \mathbf{P}_r^t \times \begin{bmatrix} \exp(j\Phi_{n,m}^{vv}) & \sqrt{\kappa}\exp(j\Phi_{n,m}^{vh}) \\ \sqrt{\kappa}\exp(j\Phi_{n,m}^{hv}) & \exp(j\Phi_{n,m}^{hh}) \end{bmatrix} \quad (4.4)$$

$\mathbf{P}_r^t$ is the polarization of the projection matrix, whose superscript and subscript are the polarization angles of the Tx antenna and Rx antenna, respectively. In our model, we have

$$\mathbf{P}_{r(90,0)}^{t(45,-45)} = \begin{bmatrix} \frac{\sqrt{2}}{2} & -\frac{\sqrt{2}}{2} \\ \frac{\sqrt{2}}{2} & \frac{\sqrt{2}}{2} \end{bmatrix} \quad (4.5)$$

It is difficult to analyze equation (2.2) due to the Hadamard product. We rewrite the channel model as follows

$$\mathbf{H} = \mathbf{H}_w \bullet \mathbf{X} = \mathbf{H}_x + \sqrt{\kappa}\mathbf{H}_z \quad (4.6)$$

where $\mathbf{H}_x$ is the ideal dual-polarized channel, and $\sqrt{\kappa}\mathbf{H}_z$ is the polarization leakage channel.

Combining (4.4) and (4.6), we have

$$\mathbf{H}_x = \sum_{n=1}^{N}\sum_{m=1}^{M} e^{-j2\pi f_i \tau_{n,m}}\mathbf{A}_{n,m} \times ((\mathbf{P}x_r^t)_{n,m} \otimes \mathbf{v}_{\theta_{n,m}}) \quad (4.7)$$

$$\mathbf{H}_z = \sum_{n=1}^{N}\sum_{m=1}^{M} e^{-j2\pi f_i \tau_{n,m}} \mathbf{A}_{n,m} \times ((\mathbf{P}z_r^t)_{n,m} \otimes \mathbf{v}_{\theta_{n,m}}) \quad (4.8)$$

where

$$(\mathbf{P}x_r^t)_{n,m} = \mathbf{P}_r^t \times \begin{bmatrix} \exp(j\Phi_{n,m}^{vv}) & 0 \\ 0 & \exp(j\Phi_{n,m}^{hh}) \end{bmatrix} \quad (4.9)$$

$$(\mathbf{P}z_r^t)_{n,m} = \mathbf{P}_r^t \times \begin{bmatrix} 0 & \exp(j\Phi_{n,m}^{vh}) \\ \exp(j\Phi_{n,m}^{hv}) & 0 \end{bmatrix} \quad (4.10)$$

Since $(\mathbf{P}x_r^t)_{n,m}$ and $(\mathbf{P}z_r^t)_{n,m}$ contain the random phase, (4.7) and (4.8) can be simplified into

$$\mathbf{H}_x = \sum_{n=1}^{N}\sum_{m=1}^{M} \mathbf{A}_{n,m} \times ((\mathbf{P}x_r^t)_{n,m} \otimes \mathbf{v}_{\theta_{n,m}}) \quad (4.11)$$

$$\mathbf{H}_z = \sum_{n=1}^{N}\sum_{m=1}^{M} \mathbf{A}_{n,m} \times ((\mathbf{P}z_r^t)_{n,m} \otimes \mathbf{v}_{\theta_{n,m}}) \quad (4.12)$$

Based on (4.6), we want to obtain the optimal Tx precoding vector, which is the right singular vectors of $\mathbf{H}$. Therefore, we investigate $\mathbf{H}^H\mathbf{H}$, whose eigenvectors are the right singular vectors of $\mathbf{H}$.

$$\mathbf{H}^H\mathbf{H} = \mathbf{H}_x^H\mathbf{H}_x + \kappa\mathbf{H}_z^H\mathbf{H}_z + \sqrt{\kappa}(\mathbf{H}_z^H\mathbf{H}_x + \mathbf{H}_x^H\mathbf{H}_z) \quad (4.13)$$

For the antenna configuration $t = (45, -45)$, $r = (0, 90)$, we can express $\mathbf{H}_x^H\mathbf{H}_x$, $\mathbf{H}_z^H\mathbf{H}_z$, $\mathbf{H}_z^H\mathbf{H}_x$, $\mathbf{H}_x^H\mathbf{H}_z$ as (4.14)∼(4.17) in Appendix A.

In our model, we decompose the channel into the ideal and non-ideal part, which is convenient for the design of feedback schemes as will be shown in the next section.

V. MULTI-COMPONENT CSI FEEDBACK SCHEMES

Recall $\mathbf{H}^H\mathbf{H}$ in (4.13), according to the analysis in Section IV, for the antenna configuration with $t = (45, -45)$ and $r = (0, 90)$, $\mathbf{H}^H\mathbf{H}$ can be expressed as

$$\mathbf{H}^H\mathbf{H} = \begin{bmatrix} \mathbf{A} & \mathbf{B} \\ \mathbf{B} & \mathbf{A} \end{bmatrix} + \kappa \begin{bmatrix} \mathbf{C} & \mathbf{D} \\ \mathbf{D} & \mathbf{C} \end{bmatrix} + \sqrt{\kappa} \begin{bmatrix} \mathbf{E} & \mathbf{F} \\ \mathbf{F} & -\mathbf{E} \end{bmatrix} \quad (5.1)$$

where the expressions for block A, B, C, D, E and F are provided as (5.17)∼(5.22) in Appendix B.

When κ is small, the last two terms in (5.1) tend to 0. However, as κ increases, the impact of the last two terms in (5.1) on the eigenvalues and eigenvectors becomes more significant. Note that channel eigenvalues monotonically increase with κ. Based on the channel model, two feedback schemes are designed for non-ideal dual-polarized channel. One is explicit feedback, which feeds back the ideal and non-ideal components of the channel directly. This scheme provides sufficient information to reconstruct $\mathbf{H}^H\mathbf{H}$ and is more efficient when the number of antenna is large. The implicit feedback scheme feeds back the components of $\mathbf{H}^H\mathbf{H}$ based on codebook, which has higher quantization efficiency.

A. EXPLICIT MULTI-COMPONENT CSI FEEDBACK SCHEME

Explicit scheme quantizes $\mathbf{H}^H\mathbf{H}$ and feeds it back. Note that the three components of $\mathbf{H}^H\mathbf{H}$ in (4.13) are all Hermitian matrices, which can be reconstructed with their eigenvalues and eigenvectors. Therefore only the eigenvalues and eigenvectors need to be fed back rather than the entire matrix. Feeding back all three matrices in (4.13) explicitly may lead to large overhead, the conventional way is to ignore the 2^{nd} and 3^{rd} matrix. Thus the channel model is simplified to

Model 1:

$$\mathbf{H}^H\mathbf{H} \approx \begin{bmatrix} \mathbf{A} & \mathbf{B} \\ \mathbf{B} & \mathbf{A} \end{bmatrix} \quad (5.2)$$

However, based on the previous analysis and simulations, Model 1 fail to consider the polarization leakage and may lead to significant performance degradation when the number of Tx antennas is large. Nevertheless, feedback design may suffer from large overhead if all the three components in (4.13) are fed back. In order to enhance performance without significantly increasing the overhead, we can abandon the 2^{nd} or 3^{rd} component in (4.13) in CSI feedback. The results are the following two models.

Model 2:

$$\mathbf{H}^H\mathbf{H} \approx \begin{bmatrix} \mathbf{A}+\kappa\mathbf{C} & \mathbf{B}+\kappa\mathbf{D} \\ \mathbf{B}+\kappa\mathbf{D} & \mathbf{A}+\kappa\mathbf{C} \end{bmatrix} \quad (5.3)$$

Model 3:

$$\mathbf{H}^H\mathbf{H} = \begin{bmatrix} \mathbf{A} & \mathbf{B} \\ \mathbf{B} & \mathbf{A} \end{bmatrix} + \sqrt{\kappa} \begin{bmatrix} \mathbf{E} & \mathbf{F} \\ \mathbf{F} & -\mathbf{E} \end{bmatrix} \quad (5.4)$$

TABLE 1. Power loss of the explicit feedback models.

XPR	Model 1 Power Loss	Model 2 Power Loss	Model 3 Power Loss	Model dexcription
-12dB	25.42%	19.11%	4.80%	Model 1 $\mathbf{H}^H\mathbf{H} \approx \begin{bmatrix} \mathbf{A} & \mathbf{B} \\ \mathbf{B} & \mathbf{A} \end{bmatrix}$
-11dB	28.65%	20.70%	5.84%	
-10dB	32.33%	22.33%	7.06%	Model 2 $\mathbf{H}^H\mathbf{H} \approx \begin{bmatrix} \mathbf{A}+\kappa\mathbf{C} & \mathbf{B}+\kappa\mathbf{D} \\ \mathbf{B}+\kappa\mathbf{D} & \mathbf{A}+\kappa\mathbf{C} \end{bmatrix}$
-9dB	36.55%	23.96%	8.50%	
-8dB	41.42%	25.58%	10.18%	
-7dB	47.09%	27.13%	12.12%	Model 3 $\mathbf{H}^H\mathbf{H} \approx \begin{bmatrix} \mathbf{A} & \mathbf{B} \\ \mathbf{B} & \mathbf{A} \end{bmatrix} + \sqrt{\kappa} \begin{bmatrix} \mathbf{E} & \mathbf{F} \\ \mathbf{F} & -\mathbf{E} \end{bmatrix}$
-6dB	53.72%	28.60%	14.33%	
-5dB	61.56%	29.93%	16.83%	
-4dB	70.91%	31.10%	19.62%	
-3dB	82.17%	32.05%	22.69%	

It can be proved that the power loss of the received signal is $\frac{\sqrt{\kappa}}{1+\sqrt{\kappa}+\kappa}$ and $\frac{\kappa}{1+\sqrt{\kappa}+\kappa}$ for Model 2 and Model 3, respectively. Compared to Model 1, whose power loss is $\frac{\kappa+\sqrt{\kappa}}{1+\sqrt{\kappa}+\kappa}$, the performance is improved. We evaluate the power loss when the number of Tx antennas is very large, so that the eigenspace of the three matrices are asymptotically orthogonal. The evaluation of the power loss for different XPRs is shown in TABLE 1.

From the above analysis, it can be seen that Model 2 and Model 3 have much smaller performance loss compared to Model 1, thus can be employed for practical feedback. According to the analysis of [22, (5.1)], the eigenspace of Hermitian matrix $\mathbf{H}_x^H\mathbf{H}_x = \begin{bmatrix}\mathbf{A} & \mathbf{B}\\ \mathbf{B} & \mathbf{A}\end{bmatrix}$ is $\mathbf{V}_x$, which can be described as follows:

$$\mathbf{V}_x = \frac{\sqrt{2}}{2}\begin{bmatrix} v_1^x & v_2^x \\ v_1^x & -v_2^x \end{bmatrix} \tag{5.5}$$

$$v_1^x = \frac{\sum_i A_i \exp(\varphi_i^x) v_{\theta_i}^H}{\text{norm}(\sum_i A_i \exp(\varphi_i^x) v_{\theta_i}^H)} \tag{5.6}$$

$$v_2^x = \frac{\sum_i A_i \exp(\phi_i^x) v_{\theta_i}^H}{\text{norm}(\sum_i A_i \exp(\phi_i^x) v_{\theta_i}^H)} \tag{5.7}$$

The two eigenvalues are

$$\lambda_1^x = \text{norm}(\sum_i A_i \exp(\varphi_i^x) v_{\theta_i}^H)^2 \tag{5.8}$$

$$\lambda_2^x = \text{norm}(\sum_i A_i \exp(\phi_i^x) v_{\theta_i}^H)^2 \tag{5.9}$$

where φ_i^x and ϕ_i^x follow a uniform distribution in the range of $[0, 2\pi]$. Therefore, we have

$$\mathbf{H}_x^H\mathbf{H}_x = V_x \sum\nolimits_x (V_x)^H \tag{5.10}$$

where $\sum_x = \text{diag}(\lambda_1^x, \lambda_2^x)$.

$\mathbf{H}_z^H\mathbf{H}_z = \begin{bmatrix}\mathbf{D} & \mathbf{C}\\ \mathbf{C} & \mathbf{D}\end{bmatrix}$ can be analyzed in a similar way to $\mathbf{H}_x^H\mathbf{H}_x$. As $(\mathbf{H}_z^H\mathbf{H}_x + \mathbf{H}_x^H\mathbf{H}_z) = \begin{bmatrix}\mathbf{E} & \mathbf{F}\\ \mathbf{F} & -\mathbf{E}\end{bmatrix}$, its eigenspace is

$$V_\chi = \frac{\sqrt{2}}{2}\begin{bmatrix} v_1^\chi & v_2^\chi \\ v_2^\chi & -v_1^\chi \end{bmatrix} \tag{5.11}$$

$$v_1^\chi = \frac{\sum_i A_i \exp(\varphi_i^\chi) v_{\theta_i}^H}{\text{norm}(\sum_i A_i \exp(\varphi_i^\chi) v_{\theta_i}^H)} \tag{5.12}$$

$$v_2^\chi = \frac{\sum_i A_i \exp(\phi_i^\chi) v_{\theta_i}^H}{\text{norm}(\sum_i A_i \exp(\phi_i^\chi) v_{\theta_i}^H)} \tag{5.13}$$

Note that V_x, V_z and V_χ have the same parameter $v_{\theta_i}^H$, which contains the direction information of the i-th ray, and A_i which contains the amplitude information of the i-th ray. Those parameters can be provided by long term and wide band feedback. Only phase parameters φ_i^x, ϕ_i^x, φ_i^z, ϕ_i^z, φ_x^χ, ϕ_i^χ in V_x, V_z, V_χ requires short term and sub-band feedback.

The specific feedback design is shown in TABLE 2.

We assume that the amplitude information A_i takes 3 bit, phase value/differential phase value takes 2 bit, direction vector takes 8 bit, and $\sqrt{\kappa}$ takes 3 bit. The overhead of feeding back the eigenvectors of $\mathbf{H}_x^H\mathbf{H}_x$ is analyzed in Appendix C.

TABLE 2. Feedback design for the parameters.

Report Type	Period	Frequency granularity	Description
$A_i \;\; i = 1, 2 \cdots N$	Long term	Wideband	Ray Power N is the number of main paths
Level 1 $\varphi_i^x - \varphi_{i-1}^x$ $i = 1 \cdots N-1$	Long term	Wideband	Construct the eigenvectors of $\mathbf{H}_x^H\mathbf{H}_x = \begin{bmatrix}\mathbf{A} & \mathbf{B}\\ \mathbf{B} & \mathbf{A}\end{bmatrix}$
Level 1 $\phi_i^x - \phi_{i-1}^x$ $i = 1 \cdots N-1$	Long term	Wideband	
Level 1 $\varphi_i^\chi - \varphi_{i-1}^\chi$ or $\varphi_i^z - \varphi_{i-1}^z$ $i = 1 \cdots N-1$	Long term	Wideband	Construct the eigenvectors of $\mathbf{H}_z^H\mathbf{H}_z = \begin{bmatrix}\mathbf{C} & \mathbf{D}\\ \mathbf{D} & \mathbf{C}\end{bmatrix}$ or $\mathbf{H}_x^H\mathbf{H}_z + \mathbf{H}_z^H\mathbf{H}_x = \begin{bmatrix}\mathbf{E} & \mathbf{F}\\ \mathbf{F} & \mathbf{E}\end{bmatrix}$
Level 1 $\phi_i^\chi - \phi_{i-1}^\chi$ or $\phi_i^z - \phi_{i-1}^z$ $i = 1 \cdots N-1$	Long term	Wideband	
Level 2 $\varphi_i^x - \varphi_{i-1}^x$ $i = 1 \cdots N-1$	Short term	Subband	Construct the eigenvectors of $\mathbf{H}_x^H\mathbf{H}_x = \begin{bmatrix}\mathbf{A} & \mathbf{B}\\ \mathbf{B} & \mathbf{A}\end{bmatrix}$
Level 2 $\phi_i^x - \phi_{i-1}^x$ $i = 1 \cdots N-1$	Short term	Subband	
Level 2 $\varphi_i^\chi - \varphi_{i-1}^\chi$ or $\varphi_i^z - \varphi_{i-1}^z$ $i = 1 \cdots N-1$	Short term	Subband	Construct the eigenvectors of $\mathbf{H}_z^H\mathbf{H}_z = \begin{bmatrix}\mathbf{C} & \mathbf{D}\\ \mathbf{D} & \mathbf{C}\end{bmatrix}$ or $\mathbf{H}_x^H\mathbf{H}_z + \mathbf{H}_z^H\mathbf{H}_x = \begin{bmatrix}\mathbf{E} & \mathbf{F}\\ \mathbf{F} & \mathbf{E}\end{bmatrix}$
Level 2 $\phi_i^\chi - \phi_{i-1}^\chi$ or $\phi_i^z - \phi_{i-1}^z$ $i = 1 \cdots N-1$	Short term	Subband	
$\sqrt{\kappa}$	Long term	Wideband	XPR information

B. IMPLICIT MULTI-COMPONENT CSI FEEDBACK SCHEME

Besides quantizing the eigenvectors of the channel matrix directly, we can also construct the optimal precoder $\mathbf{p}_{final}$ by combining several codewords selected from multiple codebooks. Note that (4.13) can be rewritten as

$$\mathbf{H}^H\mathbf{H} = \begin{bmatrix}\mathbf{A}+\kappa\mathbf{C} & \mathbf{B}+\kappa\mathbf{D}\\ \mathbf{B}+\kappa\mathbf{D} & \mathbf{A}+\kappa\mathbf{C}\end{bmatrix} + \sqrt{\kappa}\begin{bmatrix}\mathbf{F} & \mathbf{E}\\ \mathbf{E} & -\mathbf{F}\end{bmatrix} \tag{5.14}$$

For Rank-1 feedback, the upper bound is

$$\begin{aligned}
&\mathbf{E}\{\arg\min_{p\in CB}\|\mathbf{H}p\|_F^2\}\\
&\le E\left\{\arg\min_{p_1\in CB_1}\left\|p_1^H\begin{bmatrix}\mathbf{A}+\kappa\mathbf{C} & \mathbf{B}+\kappa\mathbf{D}\\ \mathbf{B}+\kappa\mathbf{D} & \mathbf{A}+\kappa\mathbf{C}\end{bmatrix}p_1\right\|_F\right\}\\
&\quad + E\left\{\arg\min_{p_2\in CB_2}\left\|p_2^H\sqrt{\kappa}\begin{bmatrix}\mathbf{F} & \mathbf{E}\\ \mathbf{E} & -\mathbf{F}\end{bmatrix}p_2\right\|_F\right\}\\
&\approx E\left\{\arg\min_{p_1\in CB_1, p_2\in CB_2}\Big\|\Gamma(p_1,p_2,\kappa,\vartheta)^H\right.\\
&\qquad\times\left(\begin{bmatrix}\mathbf{A}+\kappa\mathbf{C} & \mathbf{B}+\kappa\mathbf{D}\\ \mathbf{B}+\kappa\mathbf{D} & \mathbf{A}+\kappa\mathbf{C}\end{bmatrix}\right.\\
&\qquad\left.\left.+\sqrt{\kappa}\begin{bmatrix}\mathbf{F} & \mathbf{E}\\ \mathbf{E} & -\mathbf{F}\end{bmatrix}\right)\Gamma(p_1,p_2,\kappa,\vartheta)\Big\|_F\right\}
\end{aligned} \tag{5.15}$$

The approximation above decomposes the problem of deriving the optimal $\mathbf{p}_{opt}$ into two sub-problems, i.e., deriving

the optimal $\mathbf{p}_1$ for $\begin{bmatrix} \mathbf{A}+\kappa\mathbf{C} & \mathbf{B}+\kappa\mathbf{D} \\ \mathbf{B}+\kappa\mathbf{D} & \mathbf{A}+\kappa\mathbf{C} \end{bmatrix}$ and the optimal $\mathbf{p}_2$ for $\begin{bmatrix} \mathbf{F} & \mathbf{E} \\ \mathbf{E} & -\mathbf{F} \end{bmatrix}$. The resultant precoder $\mathbf{p}'_{opt}$ is a combination of $\mathbf{p}_1$, $\mathbf{p}_2$, Given weight phase ϑ and the weight amplitude K, the final precoding vector can be expressed as

$$p'_{opt} = \Gamma(p_1, p_2, K, \vartheta) = p_1 + Ke^{j\vartheta}p_2 \tag{5.16}$$

The two codebooks correspond to the eigenvector of different matrices. Thus the codebook models are different, which are $\begin{bmatrix} v_1^{x,z} & v_2^{x,z} \\ v_1^{x,z} & -v_2^{x,z} \end{bmatrix}$ and $\begin{bmatrix} v_1^{\chi} & v_2^{\chi} \\ v_2^{\chi} & -v_1^{\chi} \end{bmatrix}$, respectively. The codebook for each model can reuse the design methods in LTE-A. The feedback information is listed in the following TABLE 3.

TABLE 3. Design for implicit multi-components CSI feedback.

Report Type	Period	Frequency granularity	Description
Level 1 f_1	Long term	Wideband	the 1-st level information of the optimal precoder for $\begin{bmatrix} \mathbf{A}+\kappa\mathbf{C} & \mathbf{B}+\kappa\mathbf{D} \\ \mathbf{B}+\kappa\mathbf{D} & \mathbf{A}+\kappa\mathbf{C} \end{bmatrix}$
Level 2 f_1	Short term	Subband	the 2-nd level information of the optimal precoder for $\begin{bmatrix} \mathbf{A}+\kappa\mathbf{C} & \mathbf{B}+\kappa\mathbf{D} \\ \mathbf{B}+\kappa\mathbf{D} & \mathbf{A}+\kappa\mathbf{C} \end{bmatrix}$
Level 1 f_2	Long term	Wideband	the 1-st level information of the optimal precoder for $\begin{bmatrix} \mathbf{F} & \mathbf{E} \\ \mathbf{E} & -\mathbf{F} \end{bmatrix}$
Level 2 f_2	Short term	Subband	the 2-nd level information of the optimal precoder for $\begin{bmatrix} \mathbf{F} & \mathbf{E} \\ \mathbf{E} & -\mathbf{F} \end{bmatrix}$
ϑ	Short term	Subband	the weight phase
K	Long term	Wideband	the weight amplitude

We assume that $\mathbf{v}_1^{x,z}$, $\mathbf{v}_2^{x,z}$, $\mathbf{v}_1^{\chi}$, $\mathbf{v}_2^{\chi}$ takes 8bit per vector. As a result, when we don't consider the polarization leakage, the feedback overhead is 16bit. When we consider the polarization leakage, the feedback overhead is 38bit.

This scheme is suitable for channel dimensions that are not very large and scattering, when the number of effective multipath is large, such as 8, 12, 16, 32, etc.. If we use the explicit approach, the cost will be high under large N. Although the accuracy is inferior compared with the explicit scheme, the overall overhead of the implicit scheme can be controlled under reasonable budget.

VI. PERFORMANCE EVALUATION

In this section, the performance of the proposed feedback schemes are validated using simulation.

A. LINK LEVEL PERFORMANCE EVALUATION

In this sub-section, we present the results of link-level simulations. The channel is generated following the channel model in [27]. CSI is quantized with the proposed schemes, and quantization performance is evaluated by the chord distance between the quantized channel vector and the real channel vector. According to the definition, smaller chord distance means more accurate CSI and vice versa.

1) EXPLICIT MULTI-COMPONENT CSI FEEDBACK

We evaluate the performance of explicit CSI feedback Model 1, Model 2 and Model 3 under different XPR. The antenna is a uniform linear array (ULA) containing 1×32 dual-polarized antennas, which is often used in reality.

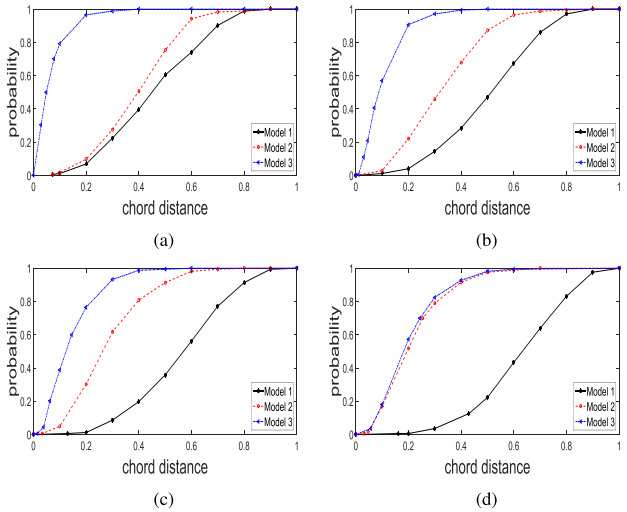

FIGURE 3. The performance of the Single/Multi-Component CSI feedback for correlated channel. (a) 64Tx, CDF of chord distance,explicit CSI feedback, XPR=8dB. (b) 64Tx, CDF of chord distance,explicit CSI feedback, XPR=5dB. (c) 64Tx, CDF of chord distance,explicit CSI feedback, XPR=3dB. (d) 64Tx, CDF of chord distance,explicit CSI feedback, XPR=0dB.

Feedback Model 1 ignores the polarization leakage, whereas feedback Model 2 and Model 3 takes polarization leakage into consideration. Since our goal is to evaluate different feedback models, ideal quantization of the multi-path amplitudes and directions are assumed. The simulation is conducted with XPR=0dB, 3dB, 5dB and 8dB, and the results for correlated and uncorrelated channels are shown in Fig. 3 and Fig. 4, respectively.

It can be observed that for correlated channels, the performance of the multi-component CSI feedback based on Model 2 and 3 is much better than single component CSI feedback based on Model 1. Moreover, when polarization leakage is large, the performance of Model 3 is very close to Model 2. However, when polarization leakage is small, Model 3 has better performance than Model 2 in Fig.3 (a), (b), (c). In general, the chord distance actually measures the loss in beamforming gain. It can be observed that for uncorrelated channels, the performance of the multi-component CSI feedback is similar to that of the correlated channel. However, compared with correlated channel, the performance gain for the uncorrelated channel is larger.

2) IMPLICIT MULTI-COMPONENTS CSI FEEDBACK

The performance of implicit feedback schemes is also evaluated. We compare the performance of the feedback approaches based on a single codebook and two codebooks.

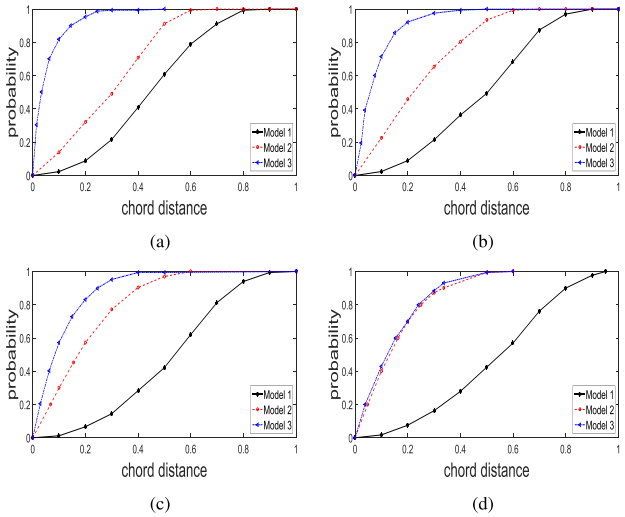

FIGURE 4. The performance of the Single/Multi-Component CSI feedback for uncorrelated channel. (a) 64Tx, CDF of chord distance,explicit CSI feedback, XPR=8dB. (b) 64Tx, CDF of chord distance,explicit CSI feedback, XPR=5dB. (c) 64Tx, CDF of chord distance,explicit CSI feedback, XPR=3dB. (d) 64Tx, CDF of chord distance,explicit CSI feedback, XPR=0dB.

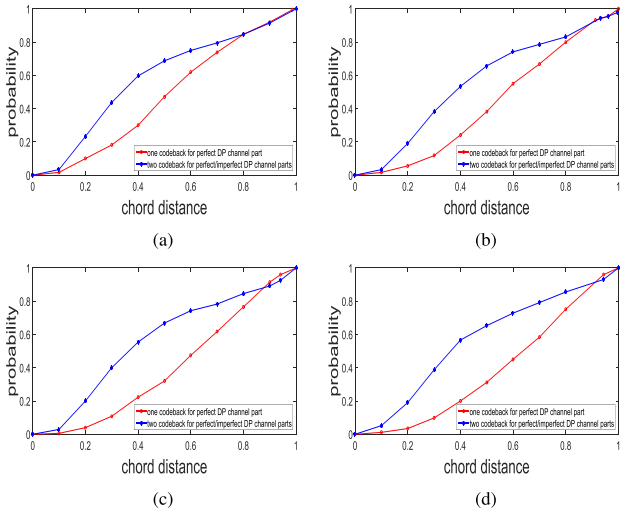

FIGURE 5. The performance of the one/two-codebook feedback for correlated channel. (a) 64Tx, CDF of chord distance,implicit CSI feedback, XPR=8dB. (b) 64Tx, CDF of chord distance,implicit CSI feedback, XPR=5dB. (c) 64Tx, CDF of chord distance,implicit CSI feedback, XPR=3dB. (d) 64Tx, CDF of chord distance,implicit CSI feedback, XPR=0dB.

The single codebook scheme corresponds to the traditional methods that does not take polarization leakage into consideration. The two codebooks follows the model $\begin{bmatrix} v_1^{x,z} & v_2^{x,z} \\ v_1^{x,z} & -v_2^{x,z} \end{bmatrix}$ and $\begin{bmatrix} v_1^{\chi} & v_2^{\chi} \\ v_2^{\chi} & -v_1^{\chi} \end{bmatrix}$, where $\mathbf{v}_1^{x,z}$, $\mathbf{v}_2^{x,z}$, $\mathbf{v}_1^{\chi}$ and $\mathbf{v}_2^{\chi}$ are 6-bit 32×1 DFT vectors for correlated channel and 8-bit random vectors for uncorrelated channel. We utilize 4 bits to quantize the phase and amplitude, respectively. The performance of the two approaches is plotted in Fig.5 and Fig.6.

For correlated channel, when the antenna number is large, single-component CSI feedback has very poor performance while multiple component CSI feedback based on two

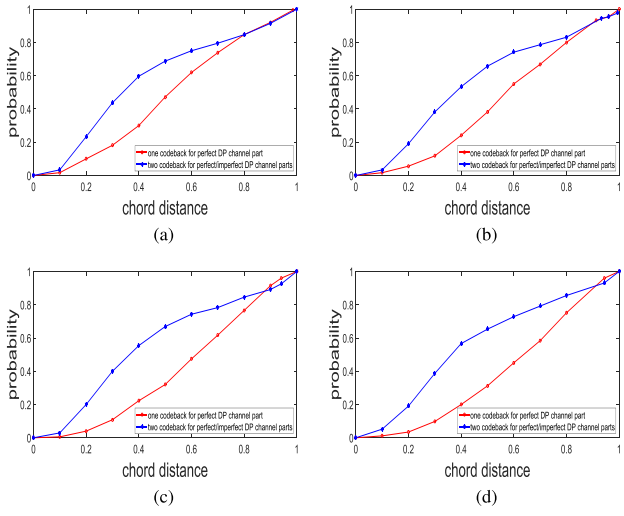

FIGURE 6. The performance of the one/two-codebook feedback for uncorrelated channel. (a) 64Tx, CDF of chord distance,implicit CSI feedback, XPR=8dB. (b) 64Tx, CDF of chord distance,implicit CSI feedback, XPR=5dB. (c) 64Tx, CDF of chord distance,implicit CSI feedback, XPR=3dB. (d) 64Tx, CDF of chord distance,implicit CSI feedback, XPR=0dB.

codebook has much better performance. For uncorrelated channel, the performance is similar to the correlated channel. Furthermore, it can be seen that since the overhead is limited, implicit feedback offers inferior performance compared to explicit feedback.

B. SYSTEM LEVEL PERFORMANCE EVALUATION

We simulate the feedback schemes under antenna topology $(M, N, P, Q) = (8, 4, 2, 64)$, where M is the number of vertical antennas, N is the number of horizontal antennas, and P=2 means dual polarization. The simulation scenario is 3D-UMi /3D-UMa. See Appendix D for more details of the simulation.

TABLE 4. Performance of single/multiple component explicit CSI feedback, Non-full buffer.

Scenario /Offered Load	CSI feedback scheme	RU	Mean UPT (Mbps)	5% UPT (Mbps)	50% UPT (Mbps)
3D-UMi Offered Load= 20Mbps	Model 1	0.74	22.69 (100%)	3.14 (100%)	19.14 (100%)
	Model 2	0.62	28.87 (127.25%)	6.93 (220.37%)	25.86 (135.12%)
	Model 3	0.58	32.86 (144.85%)	9.55 (303.57%)	32.26 (168.55%)
3D-UMa ISD 200m Offered Load= 20Mbps	Model 1	0.76	20.08 (100%)	2.54 (100%)	16.26 (100%)
	Model 2	0.64	26.88 (133.86%)	5.89 (231.89%)	23.08 (141.94%)
	Model 3	0.60	30.68 (152.79%)	8.56 (337.01%)	30.12 (185.24%)

1) EXPLICIT MULTI-COMPONENTS CSI FEEDBACK

The performance is reported in TABLE 4. It can be observed that the multiple-component CSI feedback based on Model 2 has 27.25%∼33.86% performance gain on the mean UPT and 120.37%∼131.89% performance gain on the 5% UPT. The multiple-component CSI feedback based on Model 3 has

TABLE 5. Performance of single/multiple component implicit CSI feedback.

Scenario /Offered Load	CSI feedback scheme	RU	Mean UPT (Mbps)	5% UPT (Mbps)	50% UPT (Mbps)
3D-UMi Offered Load= 20Mbps	One codebook scheme (Baseline)	0.763	20.98 (100%)	2.27 (100%)	17.46 (100%)
	Two codebook scheme	0.73	23.02 (109.72%)	2.78 (122.47%)	19.27 (110.37%)
3D-UMa ISD 200m Offered Load= 20Mbps	One codebook scheme (Baseline)	0.78	18.58 (100%)	1.84 (100%)	14.82 (100%)
	Two codebook scheme	0.64	20.88 (112.38%)	2.39 (129.89%)	17.08 (115.25%)

44.85%∼52.79% performance gain on the mean UPT and 103.57%∼137.01% performance gain on the 5% UPT.

2) IMPLICIT MULTI-COMPONENTS CSI FEEDBACK

The performance is reported in TABLE 5.

It can be observed that the multiple-component CSI feedback based on two codebook has 9.72%∼12.38% performance gain on the mean UPT and 22.47%∼29.89% performance gain on the 5% UPT.

VII. CONCLUSION

In this paper, an analytical model for dual-polarized massive MIMO with polarization leakage is formulated. The covariance matrix of the channel is decomposed into two components, i.e., the ideal polarization channel and the polarization leakage channel. On this basis, we analyze each of the two components and derive expressions of their eigenvectors, then propose explicit and implicit feedback schemes. Compared with feedback schemes for ideal polarization channel, simulation results prove the proposed schemes provide significantly improved performance with marginal increase in feedback overhead.

APPENDIX A
EXPRESSIONS OF THE TERMS IN (4.13)

Expressions (4.14)–(4.17) are shown at the bottom of this page.

APPENDIX B
EXPRESSIONS OF THE TERMS IN (5.1)

$$A = \frac{\sqrt{2}}{2} \times \sum_{n,m}^{N,M} \sum_{k,l}^{N,M} \Big(A_{n,m} A_{k,l} \times \left[\exp(j\triangle\Phi_a) + \exp(j\triangle\Phi_b) \right] v_{\theta_{n,m}}^H v_{\theta_{k,l}} \Big) \tag{5.17}$$

$$B = \frac{\sqrt{2}}{2} \times \sum_{n,m}^{N,M} \sum_{k,l}^{N,M} \Big(A_{n,m} A_{k,l} \times \left[-\exp(j\triangle\Phi_a) + \exp(j\triangle\Phi_b) \right] v_{\theta_{n,m}}^H v_{\theta_{k,l}} \Big) \tag{5.18}$$

$$C = \frac{\sqrt{2}}{2} \times \sum_{n,m}^{N,M} \sum_{k,l}^{N,M} \Big(A_{n,m} A_{k,l} \times \left[\exp(j\triangle\Phi_c) + \exp(j\triangle\Phi_d) \right] v_{\theta_{n,m}}^H v_{\theta_{k,l}} \Big) \tag{5.19}$$

$$D = \frac{\sqrt{2}}{2} \times \sum_{n,m}^{N,M} \sum_{k,l}^{N,M} \Big(A_{n,m} A_{k,l} \times \left[\exp(j\triangle\Phi_c) - \exp(j\triangle\Phi_d) \right] v_{\theta_{n,m}}^H v_{\theta_{k,l}} \Big) \tag{5.20}$$

$$E = \frac{\sqrt{2}}{2} \times \sum_{n,m}^{N,M} \sum_{k,l}^{N,M} \Big(A_{n,m} A_{k,l} \times \begin{bmatrix} \exp(j\triangle\Phi_e) + \exp(j\triangle\Phi_f) \\ + \exp(j\triangle\Phi_g) + \exp(j\triangle\Phi_h) \end{bmatrix} v_{\theta_{n,m}}^H v_{\theta_{k,l}} \Big) \tag{5.21}$$

$$H_z^H H_x = \frac{\sqrt{2}}{2} \times \sum_{n,m}^{N,M} \sum_{k,l}^{N,M} \left(A_{n,m} A_{k,l} \times \begin{bmatrix} [\exp(j\triangle\Phi_g) + \exp(j\triangle\Phi_h)] v_{\theta_{n,m}}^H v_{\theta_{k,l}} & [\exp(j\triangle\Phi_g) - \exp(j\triangle\Phi_h)] v_{\theta_{n,m}}^H v_{\theta_{k,l}} \\ [\exp(j\triangle\Phi_g) - \exp(j\triangle\Phi_h)] v_{\theta_{n,m}}^H v_{\theta_{k,l}} & -[\exp(j\triangle\Phi_g) + \exp(j\triangle\Phi_h)] v_{\theta_{n,m}}^H v_{\theta_{k,l}} \end{bmatrix} \right)$$
$$\triangle\Phi_a = \Phi_{k,l}^{vv} - \Phi_{n,m}^{vv}, \quad \triangle\Phi_b = \Phi_{k,l}^{hh} - \Phi_{n,m}^{hh} \tag{4.14}$$

$$H_z^H H_z = \frac{\sqrt{2}}{2} \times \sum_{n,m}^{N,M} \sum_{k,l}^{N,M} \left(A_{n,m} A_{k,l} \times \begin{bmatrix} [\exp(j\triangle\Phi_c) + \exp(j\triangle\Phi_d)] v_{\theta_{n,m}}^H v_{\theta_{k,l}} & [\exp(j\triangle\Phi_c) - \exp(j\triangle\Phi_d)] v_{\theta_{n,m}}^H v_{\theta_{k,l}} \\ [\exp(j\triangle\Phi_c) - \exp(j\triangle\Phi_d)] v_{\theta_{n,m}}^H v_{\theta_{k,l}} & [\exp(j\triangle\Phi_c) + \exp(j\triangle\Phi_d)] v_{\theta_{n,m}}^H v_{\theta_{k,l}} \end{bmatrix} \right)$$
$$\triangle\Phi_c = \Phi_{k,l}^{vh} - \Phi_{n,m}^{vh}, \quad \triangle\Phi_d = \Phi_{k,l}^{hv} - \Phi_{n,m}^{hv} \tag{4.15}$$

$$H_x^H H_z = \frac{\sqrt{2}}{2} \times \sum_{n,m}^{N,M} \sum_{k,l}^{N,M} \left(A_{n,m} A_{k,l} \times \begin{bmatrix} [\exp(j\triangle\Phi_e) + \exp(j\triangle\Phi_f)] v_{\theta_{n,m}}^H v_{\theta_{k,l}} & [\exp(j\triangle\Phi_e) - \exp(j\triangle\Phi_f)] v_{\theta_{n,m}}^H v_{\theta_{k,l}} \\ [\exp(j\triangle\Phi_e) - \exp(j\triangle\Phi_f)] v_{\theta_{n,m}}^H v_{\theta_{k,l}} & -[\exp(j\triangle\Phi_e) + \exp(j\triangle\Phi_f)] v_{\theta_{n,m}}^H v_{\theta_{k,l}} \end{bmatrix} \right)$$
$$\triangle\Phi_e = \Phi_{k,l}^{vh} - \Phi_{n,m}^{vv}, \quad \triangle\Phi_f = \Phi_{k,l}^{hv} - \Phi_{n,m}^{hh} \tag{4.16}$$

$$H_z^H H_x = \frac{\sqrt{2}}{2} \times \sum_{n,m}^{N,M} \sum_{k,l}^{N,M} \left(A_{n,m} A_{k,l} \times \begin{bmatrix} [\exp(j\triangle\Phi_g) + \exp(j\triangle\Phi_h)] v_{\theta_{n,m}}^H v_{\theta_{k,l}} & [\exp(j\triangle\Phi_g) - \exp(j\triangle\Phi_h)] v_{\theta_{n,m}}^H v_{\theta_{k,l}} \\ [\exp(j\triangle\Phi_g) - \exp(j\triangle\Phi_h)] v_{\theta_{n,m}}^H v_{\theta_{k,l}} & -[\exp(j\triangle\Phi_g) + \exp(j\triangle\Phi_h)] v_{\theta_{n,m}}^H v_{\theta_{k,l}} \end{bmatrix} \right)$$
$$\triangle\Phi_g = \Phi_{k,l}^{vv} - \Phi_{n,m}^{vh}, \quad \triangle\Phi_h = \Phi_{k,l}^{hh} - \Phi_{n,m}^{hv} \tag{4.17}$$

TABLE 6. 1 Simulation parameters for Macrocell Scenario.

Parameters	Assumptions
Cellular Layout	Hexagonal grid, 7 sites, 3 Macro cells per site, geographical based wrap-around
Channel Model	3D UMa ISD 200 3D UMi ISD 200
Operating bandwidth (BW)	10 MHz
Tx Power	3D UMa ISD 200: 41dBm 3D UMI ISD 200: 41 dBm
UE Speed	3km/h
Antenna configuration	Transmitter:(N,M,P=8,4,2) Receiver: 2Rx cross-polarized antenna at UE
Downtilt	3D UMa ISD 200: 104° 3D UMI ISD 200: 100°
Antenna element spacing	$(dV, dH) = (0.8\lambda, 0.5\lambda,)$
CQI/PMI reporting interval and frequency granularity	5ms for CSI,6RB
Feedback scheme	Rel-12 enhanced CSI feedback, PUSCH mode 3-2, ideal channel covariance R, PMI feedback
Delay for scheduling and AMC	6ms
Scheduler	Proportional Fair
Receiver	MMSE-IRC With non-ideal interference covariance matrix estimation by using complex Wishart distribution with 12 degrees of freedom (Model in TR36.829 with DMRS based sample covariance matrix)
HARQ Scheme	Chase Combining
Maximum number of retransmissions	4
Traffic model	FTP1,packet size 0.5M
Feedback Assumption	Non-ideal modeling of channel estimation error modeling $\widetilde{H} = \alpha(H + E)$ is used, based on DMRS for data demodulation, based on IMR for interference measurement
Handover margin	3dB

$$F = \frac{\sqrt{2}}{2} \times \sum_{n,m}^{N,M} \sum_{k,l}^{N,M} \left(A_{n,m} A_{k,l} \times \begin{bmatrix} \exp(j\triangle\Phi_e) - \exp(j\triangle\Phi_f) \\ +\exp(j\triangle\Phi_g) - \exp(j\triangle\Phi_h) \end{bmatrix} v_{\theta_{n,m}}^H v_{\theta_{k,l}} \right) \quad (5.22)$$

APPENDIX C
FEEDBACK OVERHEAD OF IMPLICIT SCHEME

$N = 2$: 1×3 bit amplitude ratio +1×2 bit phase difference+ 2 × 8 bit direction vector = 21 bits.

$N = 3$: 2×3 bit amplitude ratio + 2 × 2 bit phase difference + 3 × 8 bit direction vector = 34 bits.

$N = 4$: .....

That is to say, the overhead of feeding back the eigenvectors of $H_x^H H_x$ is 13N-5.

When we consider the polarization leakage, the expenses of constructing the eigenvectors of $H_x^H H_x$ as follows:

$N = 2$: 1×3 bit amplitude ratio + 1 × 2 bit phase difference + 2 × 8 bit direction vector + 1 × 2 bit phase difference in the polarization leakage part = 23 bits.

$N = 3$: 2×3 bit amplitude ratio + 2 × 2 bit phase difference + 3 × 8 bit direction vector + 2 × 2 bit phase difference in the polarization leakage part = 38 bits.

As a result, the expenses of constructing the eigenvectors of $H_x^H H_x$ is 15N-7.

APPENDIX D
SIMULATION SETTING FOR SYSTEM LEVEL EVALUATION

See Table 6.

REFERENCES

[1] X. Meng, J. Li, D. Zhou, and D. Yang, "5G technology requirements and related test environments for evaluation," *China Commun.*, vol. 13, no. Supplement2, pp. 42–51, 2016. [Online]. Available: https://ieeexplore.ieee.org/document/7833459/

[2] Y. Liu, X. Shi, S. He, and Z. Shi, "Prospective positioning architecture and technologies in 5G networks," *IEEE Netw.*, vol. 31, no. 6, pp. 115–121, Nov./Dec. 2017.

[3] H. Huh, G. Caire, H. C. Papadopoulos, and S. A. Ramprashad, "Achieving 'massive MIMO' spectral efficiency with a not-so-large number of antennas," *IEEE Trans. Wireless Commun.*, vol. 11, no. 9, pp. 3226–3239, Sep. 2012.

[4] W. Qianzhu, Q. Congcong, and H. Deling, "Study of massive MIMO key technologies for 5G," *Appl. Electron. Techn.*, vol. 43, no. 7, pp. 24–27, 2017.

[5] F. Rusek *et al.*, "Scaling up MIMO: Opportunities and challenges with very large arrays," *IEEE Signal Process. Mag.*, vol. 30, no. 1, pp. 40–60, Jan. 2013.

[6] D. Li, Y. Zhou, A. Yang, and S. Guo, "Optimal pilot design with CSI feedback in massive MIMO systems," in *Proc. 9th Int. Conf. Commun. Netw. China*, Aug. 2015, pp. 448–452.

[7] J. Singh, Z. Pi, and H. Nguyen, "Low-complexity optimal CSI feedback in LTE," in *Proc. IEEE Consum. Commun. Netw. Conf.*, Jan. 2013, pp. 472–478.

[8] D. J. Love, R. W. Heath, Jr., V. K. N. Lau, D. Gesbert, B. D. Rao, and M. Andrews, "An overview of limited feedback in wireless communication systems," *IEEE J. Sel. Areas Commun.*, vol. 26, no. 8, pp. 1341–1365, Oct. 2008.

[9] J. Hou, N. Yi, and Y. Ma, "Joint space–frequency user scheduling for MIMO random beamforming with limited feedback," *IEEE Trans. Commun.*, vol. 63, no. 6, pp. 2224–2236, Jun. 2015.

[10] A. Narula, M. J. Lopez, M. D. Trott, and G. W. Wornell, "Efficient use of side information in multiple-antenna data transmission over fading channels," *IEEE J. Sel. Areas Commun.*, vol. 16, no. 8, pp. 1423–1436, Oct. 1998.

[11] H. Xiao, Y. Chen, Y.-N. R. Li, and Z. Lu, "CSI feedback for massive MIMO system with dual-polarized antennas," in *Proc. IEEE 26th Annu. Int. Symp. Pers., Indoor, Mobile Radio Commun.*, Aug./Sep. 2015, pp. 2324–2328.

[12] D. J. Love and R. W. Heath, Jr., "Grassmannian beamforming on correlated MIMO channels," in *Proc. IEEE Global Telecommun. Conf. (GLOBECOM)*, vol. 1. Nov./Dec. 2004, pp. 106–110.

[13] D. J. Love, R. W. Heath, Jr., and T. Strohmer, "Grassmannian beamforming for multiple-input multiple-output wireless systems," *IEEE Trans. Inf. Theory*, vol. 49, no. 10, pp. 2735–2747, Oct. 2003.

[14] D. J. Love and R. W. Heath, Jr., "Limited feedback unitary precoding for spatial multiplexing systems," *IEEE Trans. Inf. Theory*, vol. 51, no. 8, pp. 2967–2976, Aug. 2005.

[15] J. C. Roh and B. D. Rao, "Transmit beamforming in multiple-antenna systems with finite rate feedback: A VQ-based approach," *IEEE Trans. Inf. Theory*, vol. 52, no. 3, pp. 1101–1112, Mar. 2006.

[16] J. C. Roh and B. D. Rao, "Design and analysis of MIMO spatial multiplexing systems with quantized feedback," *IEEE Trans. Signal Process.*, vol. 54, no. 8, pp. 2874–2886, Aug. 2006.
[17] A. Medra and N. T. Davidson, "Flexible codebook design for limited feedback systems via sequential smooth optimization on the Grassmannian manifold," *IEEE Trans. Signal Process.*, vol. 62, no. 5, pp. 1305–1318, Mar. 2014.
[18] J. Zhu, J. Liu, X. She, and L. Chen, "Investigation on precoding techniques in E-UTRA and proposed adaptive precoding scheme for MIMO systems," in *Proc. 14th Asia–Pacific Conf. Commun.*, Oct. 2008, pp. 1–5.
[19] K.-K. Leung, C. W. Sung, M. Khabbazian, and M. A. Safari, "Optimal phase control for equal-gain transmission in MIMO systems with scalar quantization: Complexity and algorithms," *IEEE Trans. Inf. Theory*, vol. 56, no. 7, pp. 3343–3355, Jul. 2010.
[20] B. Clerckx, Y. Zhou, and S. Kim, "Practical codebook design for limited feedback spatial multiplexing," in *Proc. IEEE Int. Conf. Commun.*, May 2008, pp. 3982–3987.
[21] R. W. Heath, Jr., T. Wu, and A. C. K. Soong, "Progressive refinement of beamforming vectors for high-resolution limited feedback," *EURASIP J. Adv. Signal Process.*, vol. 2009, no. 1, pp. 1–13, 2009.
[22] D. J. Love and R. W. Heath, Jr., "Limited feedback diversity techniques for correlated channels," *IEEE Trans. Veh. Technol.*, vol. 55, no. 2, pp. 718–722, Mar. 2006.
[23] V. Raghavan, R. W. Heath, Jr., and A. M. Sayeed, "Systematic codebook designs for quantized beamforming in correlated MIMO channels," *IEEE J. Sel. Areas Commun.*, vol. 25, no. 7, pp. 1298–1310, Sep. 2007.
[24] L. Lu, G. Y. Li, A. L. Swindlehurst, A. Ashikhmin, and R. Zhang, "An overview of massive MIMO: Benefits and challenges," *IEEE J. Sel. Topics Signal Process.*, vol. 8, no. 5, pp. 742–758, Oct. 2014.
[25] H. Tong, M. Hoshino, F. Yang, M. Xu, and D. Imamura, *Codebook Design for 3GPP LTE-Advanced*, document 110:47-52, IEICE RCS, 2010.
[26] *Investigation on Dual Polarization Channel and Codebook*, document R1-093811, 3GPP TSG RAN WG1 Meeting #58bis, Miyazaki, Japan, Oct. 2009.
[27] *Guidelines for Evaluation of Radio Interface Technologies for IMT-Advanced*, document Rep. ITU-R M.2135, ITU-R M Report, 2009.
[28] P. Soma, D. S. Baum, V. Erceg, R. Krishnamoorthy, and A. J. Paulraj, "Analysis and modeling of multiple-input multiple-output (MIMO) radio channel based on outdoor measurements conducted at 2.5 GHz for fixed BWA applications," in *Proc. IEEE Int. Conf. Commun.*, Apr./May 2002, pp. 272–276.
[29] *3rd Generation Partnership Project; Technical Specification Group Radio Access Network; Study on 3D Channel Model for LTE (Release 12)*, document 3GPP TR 36.873 V12.2.0, 2002.

FENG ZHENG received the master's degree from Xidian University and the Ph.D. degree from the Beijing University of Posts and Telecommunications (BUPT), China. She joined the School of Information and Communication Engineering, BUPT, in 2003. Her research interest is wireless communication.

YIJIAN CHEN received the B.S. degree from Central South University in 2006. He is currently a Senior Engineer with ZTE Corporation. His current research interests include massive MIMO, coordinated multi-point transmission, high-frequency communications, and channel modeling.

BOWEN PANG is currently pursuing the bachelor's degree with the International School, Beijing University of Posts and Telecommunications, China. He is involved in the research of wireless communication.

CHEN LIU is currently pursuing the bachelor's degree with the Beijing Key Laboratory of Network System Architecture and Convergence, Beijing University of Posts and Telecommunications, China. She is involved in the research of wireless communication.

SHICHUAN WANG is currently pursuing the master's degree with the Beijing Key Laboratory of Network System Architecture and Convergence, Beijing University of Posts and Telecommunications, China. She is involved in wireless communication.

DEWEN FAN is currently pursuing the bachelor's degree with the Beijing Key Laboratory of Network System Architecture and Convergence, Beijing University of Posts and Telecommunications, China. He is involved in wireless communication.

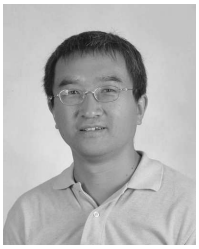

JIE ZHANG received the M.Eng. and Ph.D. degrees from the Department of Automatic Control and Electronic Engineering, East China University of Science and Technology, Shanghai, China. He joined the Communications Group, Department of Electronic and Electrical Engineering, The University of Sheffield, in 2011, as the Chair in wireless systems. His research interests cover radio propagation, indoor–outdoor radio network planning and optimization, femtocell, self-organizing network, smart building, smart city, and smart grids.